AIP | Journal of Applied Physics

Low-impedance internal linear inductive antenna for large-area flat panel display plasma processing

K. N. Kim, S. J. Jung, Y. J. Lee, G. Y. Yeom, S. H. Lee et al.

Citation: J. Appl. Phys. **97**, 063302 (2005); doi: 10.1063/1.1861136
View online: http://dx.doi.org/10.1063/1.1861136
View Table of Contents: http://jap.aip.org/resource/1/JAPIAU/v97/i6
Published by the American Institute of Physics.

Low-impedance internal linear inductive antenna for large-area flat panel display plasma processing

K. N. Kim, S. J. Jung, Y. J. Lee, and G. Y. Yeom[a)]
Department of Materials Science and Engineering, Sungkyunkwan University, Suwon, Kyunggi-do, 440-746, S. Korea

S. H. Lee and J. K. Lee
Department of Electronic and Electrical Engineering, Pohang University of Science and Technology, Pohang, 790-784, S. Korea

(Received 15 November 2004; accepted 21 December 2004; published online 4 March 2005)

An internal-type linear inductive antenna, that is, a double-comb-type antenna, was developed for a large-area plasma source having the size of 1020 mm $\times$ 830 mm, and high density plasmas on the order of 2.3×10^{11} cm^{-3} were obtained with 15 mTorr Ar at 5000 W of inductive power with good plasma stability. This is higher than that for the conventional serpentine-type antenna, possibly due to the low impedance, resulting in high efficiency of power transfer for the double-comb antenna type. In addition, due to the remarkable reduction of the antenna length, a plasma uniformity of less than 8% was obtained within the substrate area of 880 mm $\times$ 660 mm at 5000 W without having a standing-wave effect. © *2005 American Institute of Physics*. [DOI: 10.1063/1.1861136]

I. INTRODUCTION

For tens of years, semiconductor device and flat panel display (FPD) industries have adopted larger and larger area substrates in order to cut down the production cost.[1–3] In the case of thin-film transistor liquid-crystal displays (TFT-LCD), the current substrate size is in the range from 880 mm $\times$ 660 mm (fourth generation) to 1200 mm $\times$ 1000 mm (fifth generation), and it is expected to expand to larger areas within a few years.[4]

For the plasma processing of these substrates, high density plasmas are preferred due to the high production throughput and, among the various high density plasma sources, inductively coupled plasma (ICP) sources have been widely investigated due to the scalability to large area. In the case of semiconductor processing, the ICP source with external spiral-type antennas,[5,6] are generally studied, but this ICP source shows problems in the processing of the extremely large substrate size of the TFT-LCD due to the cost and thickness of its dielectric material and to the large impedance of the antennas when scaling up to larger areas. The large impedance of the antenna causes a high rf voltage on the antenna over the large area, and it can lead a low efficiency of power transfer to the plasmas by the increased capacitive coupling.[7–9]

One of the solutions resolving these problems is to use internal-type ICPs, which could effectively exclude the problems related to the thickness of dielectric materials when scaling to large areas.[10–12] Various internal-type ICPs utilizing straight antenna elements connected as serpentine shapes have been reported for large-area FPD processing.[9,11,12] However, with the increase of the substrate size, the length of the serpentine-type antenna becomes comparable to the operating rf wavelength, and the standing-wave effect that causes a nonuniform power distribution along the antenna becomes intolerable.[11]

To overcome these difficulties, an internal-type linear inductive antenna arrangement termed as "double-comb antenna" has been developed, and its plasma and processing characteristics are reported with the simulation results on the plasma characteristics.

II. EXPERIMENT

To study the characteristics of the ICP with internal-type antennas for FPD applications, a rectangular process chamber with an inner size of 1020 mm $\times$ 830 mm was fabricated. The substrate size was 880 mm $\times$ 660 mm. Five linear antennas were embedded in the process chamber and each antenna was connected to the rf power supply through the L-type matching network alternatively from the opposite ends to form a 'double-comb-type antenna'. As a comparison, the plasma characteristics of the internal linear ICP with a conventional serpentine-type antenna consisted of ten linear antennas connected in series as an S-shape were investigated. In this case, one end was connected to the matching network while the other end was connected to the ground. In the case of double comb-type antenna, the length from the matching network to the ground was about 1.2 m, while that of the serpentine-type antenna is about 13 m, which is comparable to one-half of the wavelength of 13.56 MHz rf power (about 11 m) used in this study. The details of the system used in the study can be found elsewhere.[13]

Plasma characteristics were measured using a Langmuir probe (Hiden Analytical Inc., ESP) located 7.5 cm below the antenna and along the vertical center line of the chamber. Rf voltage on the antenna was measured using a high-voltage probe (Tektronix Inc., P6015A). The etch characteristics of SiO_2 and photoresist (AZ-GXR601) films deposited on a sodalime glass were investigated using the water-cooled sub-

[a)]Electronic mail: gyyeom@skku.edu

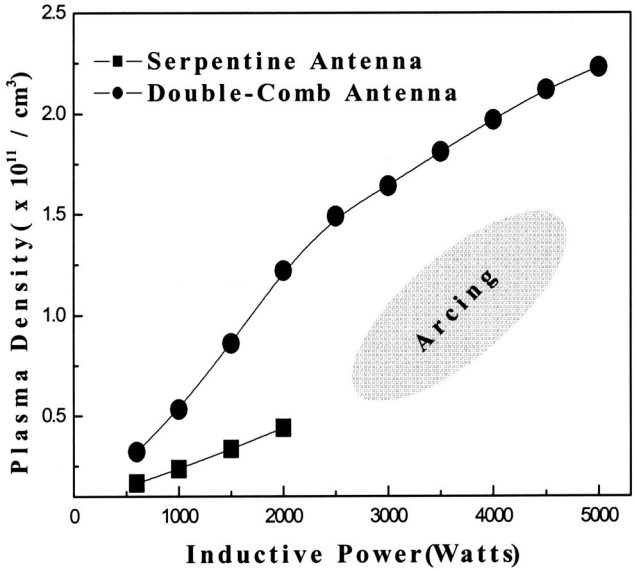

FIG. 1. Ar ion density measured by a Langmuir probe at 7.5 m below the antenna as a function of inductive power from 600 to 5000 W for 15 mTorr Ar.

strate holder installed 5 cm below the source and connected to a separate rf power supply (12.56 MHz, 0–2000 W) through a separate matching network to supply bias voltages to the substrate. A simulation of the plasma was carried out using a two-dimensional fluid code (F2L code) and was compared with the experimental data to figure out the results obtained in the experiment.

III. RESULTS AND DISCUSSION

Figure 1 shows the plasma densities measured as a function of inductive power using a Langmuir probe at 15 mTorr Ar for the two different types of linear internal antennas. As shown in the figure, the increase of inductive power to the double-comb-type antenna increased the plasma density almost linearly and high density plasma close to $2.3 \times 10^{11}/\mathrm{cm}^3$ was obtained at 5000 W of inductive power. However, in the case of the serpentine-type antenna, the plasma density was lower than that by the double-comb-type antenna, and it was difficult to measure the plasma density for the inductive power of above 2000 W due to the arcing in the chamber. Therefore, more stable and higher plasma density could be obtained with the double-comb-type antenna compared to the serpentine-type antenna.

The higher plasma density and the more stable plasma for the double-comb-type antenna are related to the lower impedance of the antenna due to the shorter antenna length. Figure 2 shows the antenna voltage measured along the antenna line from the power input to the ground for both of the antenna types at 15 mTorr Ar and 2000 W of inductive power. As shown in the figure, the measured antenna voltage was higher and showed a standing-wave effect for the serpentine-type antenna while the double-comb-type antenna showed a lower and a similar antenna voltage, indicating no standing-wave effect due to the short antenna length from the power input to the ground. Figure 2 also shows the E_z field (E_z: the induced electric field in the direction parallel to the

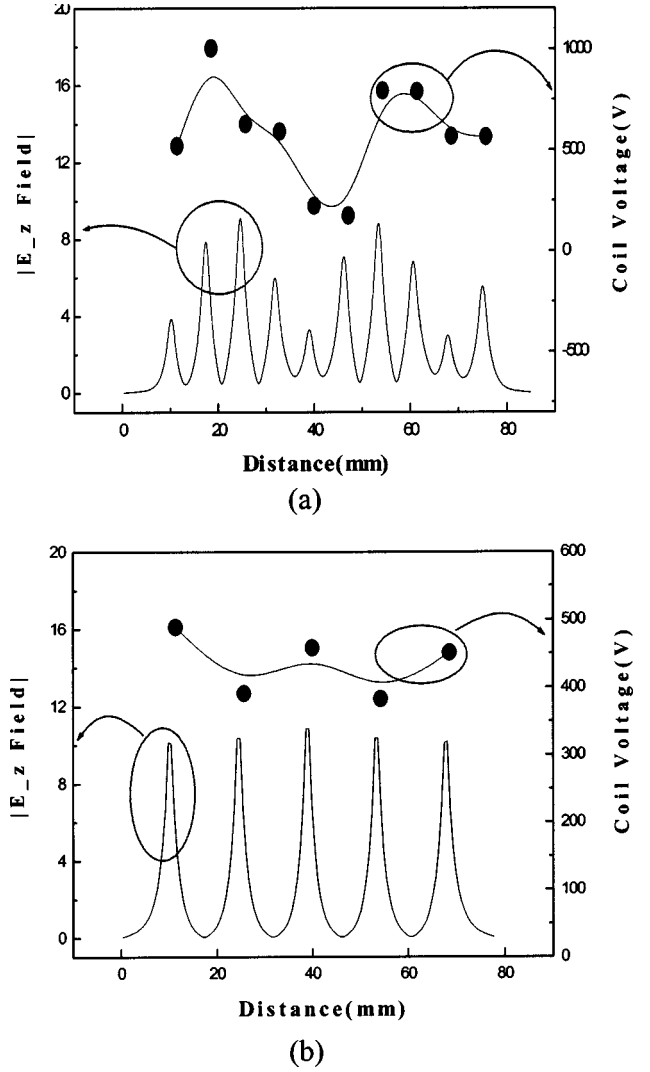

FIG. 2. Antenna voltages measured along the antenna line using a high voltage probe and the E_Z field at the each antenna position simulated by a F2L code for 2000 W and 15 mTorr Ar. (a) Serpentine-type antenna and (b) double-comb-type antenna.

antenna line) at each antenna position calculated by the F2L code. To obtain the E_z field, wave equations for the transmission line were solved to obtain the following voltage and current to the antenna:

$$V(z) = \frac{I_L}{2}[(Z_L + Z_0)e^{\gamma(l-z)} + (Z_L - Z_0)e^{\gamma(l-z)}], \tag{1}$$

$$I(z) = \frac{I_L}{2Z_0}[(Z_L + Z_0)e^{\gamma(l-z)} - (Z_L - Z_0)e^{\gamma(l-z)}], \tag{2}$$

where $V(z)$ and $I(z)$ are the voltage and current along the antenna line, respectively, Z_0 is the characteristic impedance, Z_L is the load impedance $(=(V/I)_{z=l}=(V_L/I_L)=Z_L$, l is the total antenna length), γ is the propagation constant $(=\alpha + j\beta)$, and I_L is the load current. As shown in Eqs. (1) and (2), a standing-wave effect on the current and voltage is obtained along the z direction when the $Z_0(=6.294 - 13.5564\ \Omega)$ and $\gamma(=0.0094 + j0.859\,98)$ were inserted by the calculation method suggested in the model of Wu *et al.*[14] for internal-type antennas similar to ours and when the an-

tenna length is long enough. Using Eqs. (1) and (2), the E_z fields on each of the locations of the antenna line were calculated. As shown in the figure, the E_z fields at each of the antenna locations were lower and showed the fluctuation for the serpentine-type antenna, while the double-comb-type antenna showed a higher and more uniform E_z field along the antenna line. Therefore, the higher plasma density and more stable plasma obtained with the double-comb-type antenna were related to the high and uniform current to the each antenna location.

The lack of a standing-wave effect for the DCT antenna improves the uniformity of the plasma inside the chamber. Figure 2 also shows the voltage of the antenna measured along the antenna line for both the serpentine-type antenna and double-comb-type antenna. As shown in the figure, the serpentine-type antenna showed a voltage fluctuation along the antenna line due to the standing wave effect while the double-comb-type antenna showed a similar antenna voltage. The antenna voltage can also be predicted from the voltage equation along the antenna line and showed a similar voltage fluctuation due to the reflected voltage wave. Therefore, due to the lack of a standing-wave effect, the double-comb-type antenna is believed to have inherently better plasma uniformity compared to the serpentine-type antenna.

Figure 3(a) shows the Ar plasma uniformity on the substrate area of 880 mm$\times$660 mm for the double-comb-type antenna as a function of inductive power for 15 mTorr of Ar. As shown in the figure, the uniformity of the plasma improved with increasing inductive power, from 14% for 600 W to 8% for 5000 W. Figure 3(a) also shows the calculated plasma uniformity on the substrate area. As shown in the figure, the calculated and measured uniformities showed a similar trend. The improvement of the plasma uniformity with increasing inductive power was related to the increase of plasma density near the chamber wall. On the edge of the chamber, plasma density is decreased and the variation of plasma density along the position across the antenna line can be calculated by assuming that (1) ions are immobile, (2) $N_e=N_i=N_o$ (where, N_e is electron density, N_i is ion density, and N_o is the bulk plasma density), and (3) electrons are distributed by the following Boltzmann relations:

$$N_e(x) = N_0 \times e^{e[\phi_0-\phi(x)]/kT_e}, \tag{3}$$

where ϕ_0 is the plasma potential at the center of the chamber, $\phi(x)$ is the potential along the position across the antenna, and T_e is the electron temperature. Using Poisson's equation, the $\phi(x)$ can be calculated as follows:

$$\frac{d^2\phi(x)}{dx^2} = -\frac{e}{\varepsilon_0}[N_i - N_e(x)], \tag{4}$$

$$\phi(x) = \phi_0 \frac{e^{x/\lambda_{\mathrm{De}}} - e^{-x/\lambda_{\mathrm{De}}}}{e^{l/\lambda_{\mathrm{De}}} + e^{-l/\lambda_{\mathrm{De}}}}, \tag{5}$$

$$\approx \phi_0\{e^{(x-l)/\lambda_{\mathrm{De}}} - e^{-(x+l)/\lambda_{\mathrm{De}}}\}, \tag{6}$$

where $\lambda_{\mathrm{De}}=(\varepsilon_0 kT_e/e^2N_0)^{1/2}$ is the Debye length, ε_0 is the dielectric constant, and l is the boundary position where the plasma potential start to decrease from the bulk plasma. By the application of the obtained plasma potential $\phi(x)$ to the Boltzmann equation (2), the variation of plasma density along the position across the antenna line is calculated as follows:

$$\ln\frac{N_e(x)}{N_0} = \frac{e\times\phi_0(e^{(x-l)/\lambda_{\mathrm{De}}} - e^{-(x+l)/\lambda_{\mathrm{De}}})}{kT_e}. \tag{7}$$

When the electron temperatures and bulk plasma densities were calculated as a function of inductive power for 300, 600, and 1000 W for the double-comb-type antenna with the F2L code, the obtained electron temperatures were 3.19, 3.25, and 3.42 eV, respectively, and the bulk plasma densities were 4.7×10^{10}, 9.4×10^{10}, and 1.2×10^{11} /cm^3, respectively. When the inductive power to the double-comb-type antenna is increased, the electron temperature remains similar, while the plasma density is increased significantly. Therefore, as shown in Fig. 3(a), the Debye length is decreased significantly upon increasing the inductive power. The decrease of the Debye length decreases the variation of the electron den-

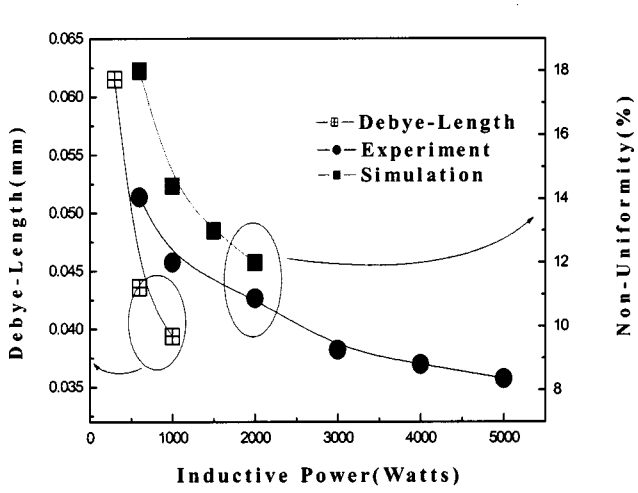

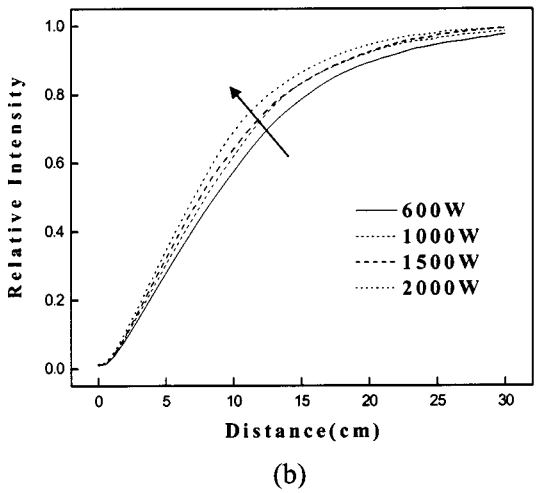

FIG. 3. (a) Plasma uniformity obtained by experiment and simulation in the double-comb antenna as a function of inductive power for the substrate area (880 mm$\times$660 mm). 15 mTorr Ar was used. (b) Plasma density distribution from 0 (chamber wall) to 30 cm calculated by the F2L code as the inductive power varies from 600 to 2000 W at 15 mTorr Ar.

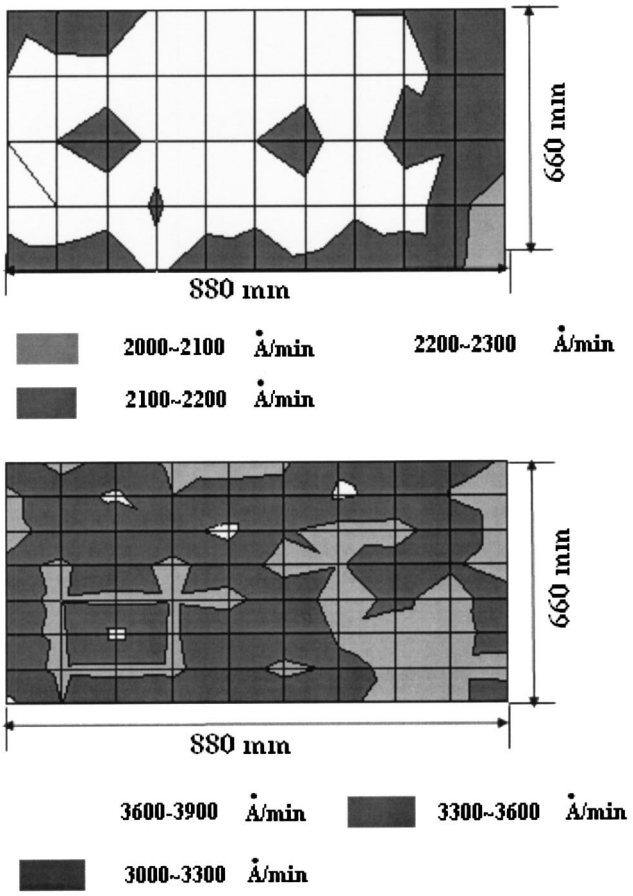

FIG. 4. (a) Etch uniformity of SiO_2 measured at 5000 W of inductive power, −35 V of dc bias voltage, and 15 mTorr of SF_6 for a substrate area of 880 mm×660 mm. (b) Etch uniformity of photoresist measured at 5000 W of rf power, −60 V of dc bias voltage, and 15 mTorr of O_2 for a substrate area of 880 mm×660 mm.

sity along the chamber position across the antenna line from Eq. (7). Figure 3(b) shows the calculated plasma density along the chamber position across the antenna line for various inductive powers for 15 mTorr Ar. As shown in the figure, the plasma density at the edge of the chamber was higher for the higher inductive power. Therefore, the improved plasma uniformity obtained for the high inductive power for the double-comb-type antenna is related to the increased plasma density near the chamber wall.

Etch uniformities on the substrate area of 880 mm ×660 mm were measured by etching SiO_2 and photoresist at 5000 W of inductive power using 15 mTorr of SF_6 and −35 V of bias voltage for SiO_2 etching, and using 15 mTorr of O_2 and −60 V of bias voltage for photoresist etching. The results are shown in Figs. 4(a) and 4(b) for SiO_2 etching and photoresist etching, respectively. As shown in the figure, the measured SiO_2 etch uniformity was about 6% with an average etch rate of 2200 Å/min and the photoresist etch uniformity was about 7% with an average etch rate of 3500 Å/min, similar to the plasma density measured with the Langmuir probe shown in Fig. 3.

IV. CONCLUSION

In summary, a internal-type linear antenna, that is, double-comb-type antenna, was compared with the serpentine-type antenna as the application to a large-area plasma source for TFT-LCD plasma processing. Due to the short antenna length of the double-comb-type antenna compared to the typical serpentine-type antenna, no standing wave effect was observed and higher and stable plasma density could be obtained. The plasma uniformity of the double-comb-type antenna was improved with increasing inductive power and it was related to the increase of plasma density near the chamber wall due to the decrease of the Debye length with increasing inductive power. By the application of 5000 W, a plasma uniformity less than 8% could be obtained on a substrate area of 880 mm×660 mm.

This work was supported by National Research Laboratory (NRL) Program of the Korea Ministry of Science and Technology.

[1] J. Holland, M. Barnes, A. Demos, T. Ni, P. Shufflebotham, and W. Yao, SID Int. Symp. Digest Tech. Papers **27**, 526 (1996).
[2] F. Heinrich, U. Banzlger, A. Jentzsch, G. Neumann, and C. Huth, J. Vac. Sci. Technol. B **14**, 2000 (1996).
[3] H. Takei, H. Kawamura, Y. Ohta, and R. Gardner, SID 98 Digest, 1998, p. 1102.
[4] J. Schmitt, M. Elyaakoubi, and L. Sansonnens, Plasma Sources Sci. Technol. **11**, A206 (2002).
[5] W. Z. Collison, T. Q. Ni, and M. S. Barnes, J. Vac. Sci. Technol. A **16**, 100 (1998).
[6] S. S. Kim, H. Y. Chang, C. S. Chang, and N. S. Yoon, Appl. Phys. Lett. **77**, 492 (2000).
[7] Z. Yu, D. Shaw, P. Gonzales, and G. J. Collins, J. Vac. Sci. Technol. A **13**, 503 (1995).
[8] J. H. Kim, H. J. Lee, Y. T. Kim, J. H. Joo, and K. W. Whang, J. Vac. Sci. Technol. A **15**, 564 (1997).
[9] T. Meziani, P. Colpo, and F. Rossi, Plasma Sources Sci. Technol. **10**, 276 (2001).
[10] K. Suzuki, K. Nakamura, H. Ohkubo, and H. Sugai, Plasma Sources Sci. Technol. **7**, 13 (1998).
[11] Y. Wu and M. A. Lieberman, Appl. Phys. Lett. **72**, 777 (1998).
[12] M. Kanoh, K. Suzuki, J. Tonotani, K. Aoki, and M. Yamage, Jpn. J. Appl. Phys., Part 1 **40**, 5419 (2001).
[13] K. N. Kim, Y. J. Lee, S. J. Jung, and G. Y. Yeom, Jpn. J. Appl. Phys., Part 1 **43**, 4373 (2004).
[14] Y. Wu and M. A. Lieberman, Plasma Sources Sci. Technol. **9**, 210 (2000).